

Structural units and low-energy configurations of [0001] tilt grain boundaries in GaN

Jun Chen*

Laboratoire Universitaire de Recherche Scientifique d'Alençon, Institut Universitaire de Technologie, 61250 Damigny, France

Pierre Ruterana and Gérard Nouet

Laboratoire d'Etude et de Recherche sur les Matériaux, FRE 2149 CNRS, Institut des Sciences de la Matière et du Rayonnement, 6 Boulevard du Maréchal Juin 14050 Caen Cedex, France

(Received 22 October 2002; published 27 May 2003)

The potential energy of $\langle 0001 \rangle$ tilt coincidence grain boundaries has been calculated using a Stillinger-Weber potential that was previously adapted to wurtzite (GaN) in order to take into account the Ga–Ga and N–N wrong bonds. The atomic structures of the grain boundaries have been determined for the lowest-energy configuration. They are described in terms of a limited number of structural units corresponding to the cores of the $\frac{1}{3}\langle 11\bar{2}0 \rangle$ edge dislocation. The potential energy curve versus tilt angle shows two energy minima for $\Sigma = 7$ and 13.

DOI: 10.1103/PhysRevB.67.205210

PACS number(s): 61.72.Mm, 68.35.–p, 68.37.–d.

I. INTRODUCTION

III–V nitride semiconductors have experienced a very fast evolution for the last decade with the fabrication of light-emitting diodes (LED's) and laser diodes (LD's).¹ These semiconductors, GaN, AlN, and InN are characterized by direct band gaps ranging from less than 1.0 eV for InN to 6.2 eV for AlN; they are highly promising in devices active from the red to the ultraviolet range of the optical spectrum. They are grown by heteroepitaxy due to the lack of suitable bulk crystals for substrates. A large variety of substrates have been tested and sapphire is now the most commonly used, although the lattice parameters and the thermal coefficient are highly mismatched. As a consequence, the layers contain large densities of threading dislocations which can reach 10^{10} cm^{-2} . Other crystallographic defects such as prismatic stacking faults, inversion domain boundaries, and nanopipes are also present. The origin of this very high density of threading dislocations is connected to the growth process resulting in a mosaic structure of slightly misoriented grains.² Thus, low-angle and high-angle grain boundaries may form and their atomic structures have been analyzed by high-resolution transmission electron microscopy (HREM).³ The atomic structure of grain boundaries has been extensively studied by HREM mainly in cubic systems.⁴

In the same way, energetic calculations have been performed on special grain boundaries described in terms of the coincidence site lattice concept in the cubic system.⁵ The description of these special grain boundaries in noncubic systems needs some approximation to take into account the nature of the parametric ratios. This approach results in the description of an experimental case by different theoretical coincidence relationship according to the chosen approximation.⁶ The introduction of the topological theory and the circuit mapping has allowed analysis of these coincidence orientations without approximation.⁷ In the case of wurtzite structure, high-resolution electron microscopy of special grain boundaries was performed in zinc oxide⁸ and gallium nitride.³ It was shown that the atomic structure of $\langle 0001 \rangle$ tilt grain boundaries in gallium nitride is based on

periodic structure involving different cores of the $\frac{1}{3}\langle 11\bar{2}0 \rangle$ edge dislocation. Atomistic simulation of these dislocation cores^{9,10} and some coincidence grain boundaries was undertaken to determine their relative stability.^{11,12} In this work, we calculated the energy of grain boundaries in the 0° – 60° range in order to determine the behavior versus the tilt angle as already reported for metals,¹³ semiconductors,¹⁴ and ceramics.¹⁵

II. INTERATOMIC POTENTIAL

The energetic calculations in nitride semiconductors dealt with the core structure of edge and screw threading dislocations using an *ab initio* local-density functional cluster method or a density functional based on the tight-binding method.^{16,17} and a density-functional–pseudopotential approach was used for stacking faults.^{18,19} These methods give accurate and reliable results but they use cells containing less than 100 atoms, which is not enough to analyze extended defects such as grain boundaries. For the latter, cells containing a large number of atoms, 500–6000, are necessary due to the length of the period of the coincidence cell unit, and empirical potentials are still the most appropriate.

Available empirical potentials have been previously used to calculate the potential energy of defects and grain boundaries in semiconductors;^{20–23} they led to a good insight for elemental semiconductors. Potentials of Keating²⁰ and of Baraff, Kane, and Schluter²¹ are limited by the surroundings; they can only deal with four-atom coordination and do not accept dangling bonds. Two other potentials, from Stillinger and Weber²² and from Tersoff,²³ which can take into account any atomic surrounding, have been widely used for III–V compound semiconductors. The treatment of compound semiconductors raises the problem of the wrong bonds, which form in crystallographic defects. In the framework of the shell-model approach, a set of interatomic potential including wrong bonds has been developed for GaN.²⁴ This potential has a rather high computing cost for large defects, so we have made a different parametrization of the Stillinger-Weber potential in order to allow a complete calculation of

TABLE I. Parameters of Stillinger-Weber potential adapted to GaN.

Parameters	Ga–N	Ga–Ga	N–N
ε (eV)	2.17	0.665	0.665
σ (nm)	0.1695	0.2038	0.1302
λ	32.5	26.76	26.76
A		7.917	
B		0.720	
a		1.8	

any atomic configuration, dangling, or wrong or excess bonds.²⁵

The Stillinger-Weber potential was initially proposed in order to analyze modifications in local order that may occur during melt in semiconductors. It is based on two terms: one for the interaction between two atoms that account for the variations of bonds lengths, and second, a three-body term, which describes the modifications of the angle between atoms. To adapt this potential to compound semiconductors, its form has been retained and only the values of some parameters were changed.²⁵ As usual, the energy is divided in two terms, the pair potential ν_2 and the three-body term ν_3 :

$$\nu_2 = \varepsilon A (B r_{ij}^{-4} - 1) \exp[(r_{ij} - a)^{-1}], \quad r_{ij} = d_{ij} / \sigma$$

where ε is the cohesive energy, d_{ij} is the length of the bond, and a is the cutoff value, and

$$\nu_3 = \varepsilon \lambda \exp[\gamma(r_{ij} - a)^{-1} + \gamma(r_{ik} - a)^{-1}] [\cos \theta_{jik} + \frac{1}{3}]^2,$$

where θ is the angle between r_i and r_j .

In such noncentrosymmetric materials, inversion domains are possible. Two models have been proposed. The Holt model is based on the exchange of anions and cations and the $\{1\bar{1}00\}$ boundary plane contains wrong bonds (Ga–Ga and N–N); small modifications of the bond lengths and small distortions of the angles are expected.²⁶ The second model is obtained by adding a translation component, $c/2$, to the inversion operation in order to eliminate these wrong bonds.^{27,28} This translation changes the atomic structure of the interface; it gives rise to 4- and 8-atom rings with different bond lengths and angles. In our case, the optimization of the parameters was carried out for the Ga–N bonds on the elastic constants to fit with the experimental data obtained by Polian, Grimsditch, and Grzegohy.²⁹ For the wrong bonds, the interaction parameters were obtained after fitting with the *ab initio* calculation of the Holt model,²⁷ and the final set is reported in Table I.²⁵ In fact, three sets are used according to the type of bonds. On this basis, the increase of the parameter λ is justified by the best fit of the elastic constants for wurtzite GaN. For the Ga–Ga bond, the bulk modulus of a gallium crystal was taken as a reference, from these parameters a value of 134 GPa is obtained with respect to 66.9 GPa by the local density approximation (LDA) calculation.³⁰ These values obtained with the Stillinger-Weber potential are acceptable by comparison to those deduced from *ab initio* calculation⁸ (Table II).

TABLE II. Energy values (mJ/m²) for the two models of inversion domain boundaries (IDB).

	<i>Ab initio</i> ^a	This work
IDB with wrong bonds	2663	2361
IDB without wrong bonds	400	567

^aReference 27.

Systematic variations of the cohesive energy and cutoff radius for the Ga–Ga and N–N bonds shows that the energy of the Holt model is in the range 1400–2800 mJ/m² for $0.265 < \varepsilon < 1.2$ eV and for $0.16 < a < 0.19$ nm. Similar modification of the parameters has been recently used to calculate the energy of dislocation cores in GaN (Ref. 10) (Table III).

As can be noticed, the values of the core energy are sensitive to the choice of the parameters. For the first choice,⁹ the three cores are distinguished, whereas in the second,¹⁰ the energy is the same for two configurations (4- and 8-atom ring). These results confirm that the capacities of empirical potentials are quite limited. However, even if the absolute value of the energy may not be reached in such calculations, the results may show the hierarchy and allow understanding the behavior of the energy of grain boundaries versus the tilt angle.³¹

The relaxation was performed using the Verlet molecular dynamic scheme³² and the defect energy was derived as the excess with respect to the bulk crystal. $E_{0\text{GaN}}$, $E_{0\text{GaGa}}$, and $E_{0\text{NN}}$ are the reference energies of the various bonds. In the calculations, we have taken -4.43 , -1.33 , and -1.33 eV, respectively. These values correspond to the minimum of the energies for the Ga–N, Ga–Ga, and N–N bonds optimized for our modified Stillinger-Weber potential. Of course, $E_{0\text{GaGa}}$ and $E_{0\text{NN}}$ are only used in cores where wrong bonds are located: we have

$$\Delta E = E - n_{\text{GaN}} E_{0\text{GaN}} - n_{\text{GaGa}} E_{0\text{GaGa}} - n_{\text{NN}} E_{0\text{NN}},$$

where E is the total energy calculated with the three parameterizations, $E_{0\text{GaN}}$, $E_{0\text{GaGa}}$, and $E_{0\text{NN}}$ are the reference energies of possible bondings, and n_{GaN} , n_{GaGa} , and n_{NN} are the number of specific bonds.

Each supercell contains two identical grain boundaries and the periodic condition is applied in the three directions. The size of the cell containing the grain boundary varies from 416 atoms for $\Sigma = 7$ with a 57-atom ring configuration

TABLE III. Energy of the core of the $\frac{1}{3}\langle 11\bar{2}0 \rangle$ edge dislocation for two parameterizations of the Stillinger-Weber (SW) potential and for the *ab initio* calculation (eV/Å).

	SW ^a	SW ^b	Elsner ^c
5/7	0.45	1.46	
8	0.785	1.72	2.19
4	1.017	1.72	

^aReference 9.

^bReference 10.

^cReference 16.

TABLE IV. The smallest rotation angles around $\langle 0001 \rangle$ for $\Sigma < 100$; the values for $[0001]$ are shown in bold.

Σ	91a	61	37	91b	73	19	43	49	31	7	67	79	13	97
Θ°	6.01	7.34	9.43	10.42	11.64	13.17	15.18	16.43	17.90	21.78	24.43	26.00	27.80	29.41
uvw	0001	0001	0001	000 $\bar{1}$	000 $\bar{1}$	0001								
Θ°	53.99	52.66	50.57	49.58	48.36	46.83	44.82	43.57	42.10	38.21	35.57	34.00	32.20	30.60
uvw	000 $\bar{1}$	000 $\bar{1}$	000 $\bar{1}$	0001	0001	000 $\bar{1}$								

to more than 5500 atoms for $\Sigma = 91b$ with a $57^+ 657^- 66666$ atomic structure for the period of the unit cell (5, 7, and 6 are the numbers of atoms forming defectuous rings for 5 and 7, and perfect rings of the wurtzite structure, 6).

III. COINCIDENCE GRAIN BOUNDARIES

Two adjacent grains may be described by a geometrical transformation such as a rotation. The introduction of the interface or grain boundary needs more parameters in order to define the indices of the interface plane and its position with respect to an origin.⁴ The character (tilt, twist, or mixed) is given by the relative position of the rotation axis with respect to the grain boundary plane (parallel, normal, or intermediate). The wurtzite structure corresponds to two hcp lattices translated along the $\langle 0001 \rangle$ axis by \mathbf{u} . In the concept of the coincidence site lattice (CSL),³³ the formation of a three-dimensional (3D) superlattice is linked to the parametric ratios except for the cubic system which is isometric. In the hexagonal system, only the rotations about $\langle 001 \rangle$ and $\langle uv0 \rangle$ axes are independent of the c/a ratio. These CSL's are characterized by an index Σ corresponding to the ratio of the unit cells of the crystal and CSL. Different methods have been proposed to calculate the possible rotations for the different Σ . Thus, it is possible to list the different descriptions with the smallest rotation angle Θ as well as their eleven equivalents for an upper limit of Σ using a generation function³⁴ (Table IV). We notice that two different descriptions are only possible in the case of $\Sigma = 91$: $\Sigma = 91a/\Theta = 6.01^\circ$ and $91b/\Theta = 10.42^\circ$. Moreover, due to the hexagonal symmetry, $P6/m\ mm$, which includes a sixfold rotation axis parallel to $[0001]$, the smallest angle is lower than 30° with $\Theta = \Theta \pm 60^\circ$. Among the twelve equivalent descriptions six correspond to rotations around $\langle 0001 \rangle$ and six to rotations around $\langle uv0 \rangle$ in the basal plane. The rotation angles around $\langle 0001 \rangle$ are complementary to 60° , and all those around $\langle uv0 \rangle$ are equal to 180° .³⁵ Therefore, the planes $\{hk0\}$ normal to the $\langle uv0 \rangle$ rotation axes are mirror planes (Table V).

Knowing the orientation relationship describing two adjacent grains, the dichromatic complex may be drawn;³⁶ it is a projection of the two crystals connected by any rotation. For GaN, the space group is $P6_3\ mc$ and the space group of the

dichromatic complexes corresponding to coincidence orientations around $[0001]$ is $P6_3\ m'c'$. The twelve symmetry operations of this group are divided into two classes: six around $[0001]$, 1, (3+), (3-), $(2+c/2)$, $[(6+)+c/2]$, and $[(6-)+c/2]$; and six around $\langle uv0 \rangle$, m' and $(c'+c/2)$. The complementary complexes for Θ and $60^\circ - \Theta$ differ by the position of their c' and m' symmetry planes. We may note that the introduction of a $c/2$ translation transforms any complex into its complementary for the same rotation angle.³ The final step of the construction of the bicrystal consists in introducing the boundary plane in the dichromatic complex before deleting one half of each crystal. As outlined previously,³⁷ the introduction of the boundary plane needs some care because the wurtzite structure exhibits corrugated planes that have two spacing, the interface can thus be located in the shuffle a , glide position b , or a combination of both. Thus, three atomic configurations must be constructed: a/a , b/b , and a/b . Only stoichiometric structures are analyzed.

For every configurations the lowest energy was calculated and the γ surface was constructed by taking into account the translations parallel and normal to the grain boundary plane.³⁸ These translations are limited to the Wigner-Seitz cell of the displacement shift lattice equivalent to the cell of nonidentical displacements.³⁹ Within such a cell, all the possible translations leaving the bicrystal unchanged have been considered. In this analysis, the translations were carried out along O_X , in the boundary plane and along O_Z , parallel to $[0001]$. The steps were $0.1a_0$ ($a_0 = 0.318$ nm) and $0.1c$ ($c = 0.519$ nm), respectively. In the third direction, O_Y normal to the boundary plane the configuration was relaxed. The energy of $\langle 0001 \rangle$ tilt boundaries was calculated for 14 Σ corresponding to rotation angles between 0° and 60° .

IV. RESULTS

A. Atomic configuration of the grain boundaries

Using geometric considerations, three types of dislocation cores, 57-, 8-, and 4-atom rings, are easily generated for the $\frac{1}{3}\langle 11\bar{2}0 \rangle$ edge dislocation with its line along the c axis. Experimental HRTEM observations show 57- and 8-atom cores

TABLE V. Twelve equivalent descriptions for $\Sigma = 7$.

	1	2	3	4	5	6	7	8	9	10	11	12
Θ (deg)	180	180	180	180	180	180	21.78	38.21	81.77	98.21	141.79	158.21
$uv0$	310	$1\bar{2}0$	$2\bar{3}0$	$1\bar{5}0$	$4\bar{1}0$	$5\bar{4}0$	001	00 $\bar{1}$	001	00 $\bar{1}$	001	00 $\bar{1}$

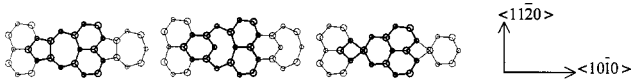


FIG. 1. $\Sigma=7$: Projection along $[0001]$ of the possible atomic structures with the three atomic cores of the $\frac{1}{3}\langle 11\bar{2}0 \rangle$ edge dislocation: 57-, 8-, and 4-atom rings.

for isolated dislocations⁴⁰ and the three cores in the grain boundaries.³ Our present investigation confirms this tendency, the reconstructed grain boundary (GB) structures contain only the three dislocation cores. We previously showed that the 57-atom dislocation core has the lowest strain energy and the 4-atom-ring dislocation the highest energy.⁹ Thus, these three cores may be used to describe the atomic structure of the grain boundaries, for instance, $\Sigma=7$ (21.79°) may exhibit three configurations (Fig. 1).

In the following, we consider the smallest period for every GB that has the minimum energy. It is shown that whatever the rotation angles, the configuration presenting the lowest energy comes from the initial configuration *aa* and as expected, the cores of the grain boundary dislocations are described by the 57-atom ring that exhibits the lowest energy for the isolated edge $\frac{1}{3}\langle 11\bar{2}0 \rangle$ dislocations.⁹ To construct the atomic models of the grain boundaries, we use this 57-atom ring in addition to regular six-atom rings of the perfect crystal.

1. Rotation angles: $0^\circ < \Theta < 21.79^\circ$

In this range, six coincidence grain boundaries have been analyzed, and all of them, except $\Sigma=7$, may be regarded as low-angle grain boundaries formed by the introduction of one 57-atom core of the edge dislocation $\frac{1}{3}[11\bar{2}0]$ or a_1 from $\Sigma=91$ ($\Theta=6.01^\circ$) to $\Sigma=19$ ($\Theta=13.17^\circ$). The next coincidence orientation, $\Sigma=49$ ($\Theta=16.43^\circ$), needs two edge dislocations per period, 57576; thus the Burgers vector of this period is $b=2a_1$ instead of $b=a_1$ for the preceding Σ 's. If we consider that 6 is the basic structural unit for the perfect crystal and 57 that for $\Sigma=7$, the intermediate coincidence grain boundaries may be described by a combination of the two units that have the lowest energies, 0 and 820 mJ/m^2 , respectively (Fig. 2). These grain boundaries are symmetric with respect to the grain boundary plane.

For $\Sigma=7$, the grain boundary is constructed with the same 57-atom ring per period. This period is the shortest (0.831 nm); this means that interaction between the cores due to overlapping of their strain field is expected. As a consequence, the energy of the grain boundary is no longer described by the continuum elastic theory, and the energy ($E_p=820 \text{ mJ/m}^2$) decreases below that of $\Sigma=49$ (Table VI).

2. Rotation angles: $21.79^\circ < \Theta < 32.20^\circ$

Beyond $\Sigma=7$, we deal with a new configuration based on two classical 57-atom rings, one shifted with respect to the other by d_{hkl} , the reticular distance of the grain boundary plane, leading to a zigzag configuration (57/57) (Fig. 3). These grain boundaries are no longer symmetric. The $\Sigma=79$ and 97 are a mixture of the previous core, 57, and of

Σ	Structural unit
1	
91a	
61	
37	
19	
49	
7	

FIG. 2. Structural unit from $\Theta=0^\circ$ to 21.79° based on the 6- and 57-atom rings; the reference structures are shown in bold.

this new unit (57/57). The Burgers vector is the same for both cores of this new unit (a_1); thus its total Burgers vector is $2a_1$. The period contents are $4a_1$ and $5a_1$ for $\Sigma=79$ and 97, respectively. For the tilt angle of 32.20° , $\Sigma=13$, a second minimum energy configuration appears, 753 mJ/m^2 , only made of the new structural unit (57/57). If a $c/2$ component is added a new configuration is obtained for the boundary, (57^+57^-) [Fig. 4]. The main difference with the previous one is the location of the wrong bonds, Ga–Ga and N–N, which are now present in the same unit period. Its energy is about the same: 764 mJ/m^2 . Each atom ring (57^+ and 57^-) is characterized by different Burgers vectors, $-a_1$ and a_2 , which are not normal to the grain boundary plane, and the total Burgers vector is $[01\bar{1}0]$ with a magnitude of $av\sqrt{3}$ (Table VI). The Burgers vectors of $(57/57)$ and (57^+57^-) units are $2a$ and $av\sqrt{3}$, respectively. Since the length of the period is the same for the two descriptions, $d=0.1136 \text{ nm}$, using the equation $2 \sin(\Theta/2)=b/d$, we obtain 0.561 and 0.486 for $2a$ and $av\sqrt{3}$, respectively, whereas the first term is 0.480. Therefore, the second atomic ring (57^+57^-) fits with the rotation and may be used to describe $\Sigma=13$.

3. Rotation angles: $32.20^\circ < \Theta < 60^\circ$

This range is characterized by a systematic introduction of the component $\Delta z=0.5$, which gives rise to the structural unit (57^+57^-) . The next boundary, $\Sigma=67$, is based on two units of $\Sigma=13$ plus one 6-atom ring, so the magnitude of the associated Burgers vector is still $2av\sqrt{3}$. The other configurations up to 60° are described by the introduction of a variable number of 6-atom rings leading to configurations of the type: $(57^+ x 6 57^- y 6)$ with x and y the number of 6-atom rings: in the range 1–3 depending on the Σ value. Since only one unit (57^+57^-) is involved for each Σ , all Burgers vectors are $[10\bar{1}0]$ with the magnitude $av\sqrt{3}$ (Table VI). These grain

TABLE VI. Description of the tilt boundaries; the basic structural units are shown in bold. E_p is the potential energy of the grain boundary in mJ/m^2 ; $a=0.318 \text{ nm}$, $c=0.519 \text{ nm}$.

Grain boundary plane	Θ (deg)	Σ	E_p (mJ/m^2)	Translation		Structure	Burgers vector \mathbf{b}
				Δx (a)	Δz (c)		
	0	1	0	0 0		6	a
$65\bar{1}\bar{1}0$	6.01	91a	721	0.9 0		576666	a
$54\bar{9}0$	7.36	61	791	0.9 0		57666	a
$43\bar{7}0$	9.43	37	858	0.9 0		5766	a
$52\bar{7}0$	13.17	19	912	0.9 0		576	a
$53\bar{8}0$	16.43	49	993	0.9 0		57576	$2a$
$21\bar{3}0$	21.79	7	820	0.9 0		57	a
73100	26.01	79	949	1.8 0		5757(57/57)	$4a$
83110	29.41	97	906	1.8 0		57(57/57)(57/57)	$5a$
$31\bar{4}0$	32.20	13	753	1.8 0		(57/57)	2a
$31\bar{4}0$	32.20	13	764	0.7 0.5		(57⁺57⁻)	$a\sqrt{3}$
92110	35.60	67	946	0.7 0.5		(57 ⁺ 57 ⁻)(57 ⁺ 57 ⁻)6	$2a\sqrt{3}$
$51\bar{6}0$	42.10	31	992	0.7 0.5		57 ⁺ 657 ⁻ 6	$a\sqrt{3}$
$61\bar{7}0$	44.82	43	1028	0.7 0.5		57 ⁺ 657 ⁻ 66	$a\sqrt{3}$
$81\bar{9}0$	48.36	73	1006	0.7 0.5		57 ⁺ 6657 ⁻ 666	$a\sqrt{3}$
91100	49.60	91b	978	0.7 0.5		57 ⁺ 66657 ⁻ 666	$a\sqrt{3}$
	60	1	0	0 0.5		6	

boundaries may be considered as low-angle grain boundaries with respect to $\Sigma = 1$ ($\Theta = 60^\circ$). The 60° rotation also needs the addition of the $c/2$ component to restore the perfect crystal of the wurtzite structure, which is connected to $\Sigma = 1$ ($\Theta = 60^\circ$) by a rotoinversion (Fig. 4).

B. The boundary energy

The variation of the energy as a function of the rotation angle presents two well-pronounced minima or energy cups corresponding to $\Sigma = 7$ ($\Theta = 21.79^\circ$) and 13 ($\Theta = 32.20^\circ$) (Fig. 5). For the angles close to 0° and 60° the continuum elasticity theory may be used to calculate the boundary energy:

$$E = E_0 \Theta \{ \Theta (\pi R/b) \coth(\pi R/b) - \ln[2 \sinh(\pi R/b)] \},$$

$$E_0 = \mu b / 4\pi(1 - \nu),$$

where R is the cutoff radius of the edge dislocation.

A good agreement is obtained in the ranges $0^\circ - 18^\circ$ and $42^\circ - 60^\circ$, which correspond to the formation of low-angle

Σ	Structural unit
7	
79	
97	
13	

FIG. 3. Structural unit from $\Theta = 21.79^\circ$ to 32.20° based on the 57- and (57/57)-atom rings leading to a zigzag configuration; the reference structures are shown in bold.

Σ	Structural unit
13	
67	
31	
43	
73	
91b	
1	

FIG. 4. Structural unit from $\Theta = 32.20^\circ$ to 60° based on the (57⁺57⁻)- and 6-atom rings; the reference structures are shown in bold.

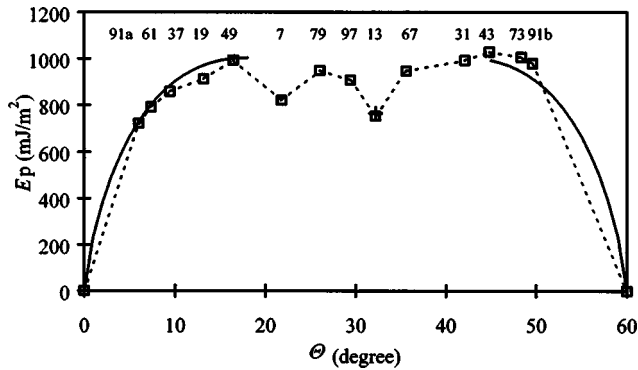


FIG. 5. Variation of the potential energy E_p of the grain boundaries as function of the rotation angle Θ with the corresponding Σ value. The solid curve is the fit with the continuum elasticity theory.

grain boundaries with respect to the perfect crystal, 0° , and to a perfect crystal after a rotation of 60° plus an inversion. The best fit with the calculated energy curve is obtained with $E_0 = 3550 \text{ mJ/m}^2$ and $R = 0.6b$.

The formation of energy minima corresponds to well-defined atomic structures of the grain boundaries with the shortest period. In these cases, the atomic structure of the grain boundary is well ordered and its coherence is high. This leads to the minimization of the dislocation strain fields. The energy of the boundary is only due to the contribution of each atomic core. The ratio of the length of the period to the magnitude of the Burgers vector shows that the zigzag configurations are needed for the largest rotation angle.

IV. DISCUSSION AND CONCLUSION

Using the modified Stillinger-Weber empirical potential, it is shown that the atomic structure of grain boundaries for $[0001]$ tilt grain boundaries can be described by a limited

number of structural units corresponding to the core of the $\frac{1}{3}\langle 11\bar{2}0 \rangle$ edge dislocation. In agreement with the results that were recently reported for the threading dislocations in GaN,^{9,10} as well as earlier experimental reports,³ three structural units, 4-, 57-, and 8-atom rings, are possible for the $\frac{1}{3}\langle 11\bar{2}0 \rangle$ edge dislocation, with the 57-atom exhibiting the lowest energy.^{9,10} The investigation of the grain boundaries was carried out using the 57-atom configuration, in combination with the 6-atom ring of the hexagonal unit. Until $\Sigma = 7$ (21.79°), it is shown that linear combinations of the two atom cycles leads to configuration of minimum energy. Beyond $\Sigma = 7$, the configurations of minimum energy are shown to have a zigzag structure, with no translation along the c axis. In this case, the total Burgers vector of the CSL depends on the number of these structural units. The turning point is reached at with $\Sigma = 13$. Above, the reconstruction of the boundaries needs the introduction of a $c/2$ translation and two variants (57^+ and 57^-) are found to lead to minimum energy configurations. It is then shown that in wurtzite GaN, the potential energy of $[0001]$ tilt grain boundaries exhibits a similar behavior that in cubic materials.⁵ Among the analyzed fourteen cases ($\Sigma < 100$) around the $\langle 0001 \rangle$ axis, a minimum of energy is shown to occur for $\Sigma = 7$ and 13. This is in contrast to the results that were very recently reported following a rather similar procedure, in which no minimum was reported in particular for $\Sigma = 7$. This was probably due to the use of nonoptimized combinations of atom cycles for the reconstruction of the boundaries.⁴¹ In the low-angle part close to 0° and 60° the energy variation follows clearly the continuum elasticity theory.

ACKNOWLEDGMENT

The authors acknowledge the support of the EU under Contract No. HPRN-CT-1999-00040.

*Author to whom correspondence should be addressed. Email address: jchen@iutalencon.unicaen.fr

¹S. Nakamura, M. Senoh, N. Iwasa, and S. Nagahama, *Jpn. J. Appl. Phys., Part 1* **34**, 1797 (1995).

²X. J. Ning, F. R. Chien, P. Pirouz, J. W. Wang, and M. A. Khan, *J. Mater. Sci.* **3**, 580 (1996).

³V. Potin, P. Ruterana, G. Nouet, R. C. Pond, and H. Morkoç, *Phys. Rev. B* **61**, 5587 (2000).

⁴A. P. Sutton and R. W. Balluffi, *Interfaces in Crystalline Material* (Clarendon, Oxford, 1995).

⁵M. Kohyama, *Modell. Simul. Mater. Sci. Eng.* **10**, R31 (2002).

⁶F. R. Cheng and A. King, *Philos. Mag. A* **57**, 431 (1988).

⁷R. C. Pond, in *Dislocations in Solids*, edited by F. R. N. Nabarro (North Holland, Amsterdam, 1989), Vol. 8, p. 1.

⁸F. Sarrazit, E. A. Stepanov, E. Olsson, T. Claeson, V. I. Bondarenko, R. C. Pond, and N. A. Kiselev, *Philos. Mag. A* **76**, 633 (1997).

⁹J. Chen, P. Ruterana, and G. Nouet, *Mater. Sci. Eng., B* **82**, 117 (2001).

¹⁰A. Béré and A. Serra, *Phys. Rev. B* **65**, 205323 (2002).

¹¹J. Chen, G. Nouet and P. Ruterana, *Phys. Status Solidi B* **228**, 411 (2001).

¹²A. Béré and A. Serra, *Interface Sci.* **9**, 149 (2001).

¹³G. C. Hasson, M. Biscondi, P. Lagarde, J. Levy and C. Goux, in *The Nature and Behavior of Grain Boundaries*, edited by H. Hu (Plenum, New York, 1972), p. 3.

¹⁴M. Kohyama, R. Yamamoto and M. Doyama, *Phys. Status Solidi* **137**, 11 (1986); **138**, 387 (1986).

¹⁵D. Wolf, *J. Am. Ceram. Soc.* **67**, 1 (1984).

¹⁶J. Elsner, R. Jones, P. K. Sitch, V. D. Porezag, M. Elstner, Th. Frauenheim, M. I. Heggie, S. Oberg, and P. R. Briddon, *Phys. Rev. Lett.* **79**, 3672 (1997).

¹⁷A. F. Wright and U. Grossner, *Appl. Phys. Lett.* **73**, 2751 (1998).

¹⁸C. Stampfl and C. G. Van de Walle, *Phys. Rev. B* **57**, R15 052 (1998).

¹⁹J. A. Chislom and P. D. Bristowe, *J. Phys.: Condens. Matter* **11**, 5067 (1999).

²⁰P. N. Keating, *Phys. Rev.* **145**, 637 (1966).

²¹G. A. Baraff, E. D. Kane, and M. Schluter, *Phys. Rev. B* **21**, 5662 (1980).

²²F. H. Stillinger and T. A. Weber, *Phys. Rev. B* **31**, 5262 (1985).

²³J. Tersoff, *Phys. Rev. B* **37**, 6991 (1988); **38**, 9902 (1988); **39**, 5566 (1989); *Phys. Rev. Lett.* **61**, 2879 (1988).

- ²⁴P. Zapol, R. Pandey and J. D. Gale, *J. Phys.: Condens. Matter* **9**, 9517 (1997).
- ²⁵N. Aïchoune, V. Potin, P. Ruterana, A. Hairie, G. Nouet, and E. Paumier, *Comput. Mater. Sci.* **17**, 380 (2000).
- ²⁶D. B. Holt, *J. Phys. Chem. Solids* **30**, 1297 (1969).
- ²⁷J. E. Northrup, J. Neugebauer, and L. T. Romano, *Phys. Rev. Lett.* **77**, 103 (1996).
- ²⁸V. Potin, P. Ruterana, and G. Nouet, *J. Appl. Phys.* **82**, 2176 (1997).
- ²⁹A. Polian, M. Grimsditch, and J. Grzegory, *J. Appl. Phys.* **79**, 3343 (1996).
- ³⁰M. Bernasconi, G. L. Chiarotti, and E. Tosatti, *Phys. Rev. B* **52**, 9988 (1995).
- ³¹J. T. Wetzell, A. A. Levi, D. A. Smith, *Trans. Jpn. Inst. Met.* **27**, 1060 (1986).
- ³²L. Verlet, *Phys. Rev.* **159**, 98 (1967).
- ³³W. Bollmann, *Crystal Defects and Crystalline Interfaces* (Springer, Berlin, 1970).
- ³⁴G. L. Bleris, G. Nouet, S. Hagege, and P. Delavignette, *Acta Crystallogr., Sect. A: Cryst. Phys., Diffr., Theor. Gen. Crystallogr.* **38**, 550 (1982).
- ³⁵S. Hagege and G. Nouet, *Acta Crystallogr., Sect. A: Found. Crystallogr.* **45**, 217 (1989).
- ³⁶R. C. Pond and D. S. Vlachavas, *Proc. R. Soc. London, Ser. A* **386**, 95 (1983).
- ³⁷F. Oba, I. Tanaka, S. R. Nishitani, H. Adachi, B. Slater, and D. H. Gay, *Philos. Mag. A* **80**, 1567 (2000).
- ³⁸V. Vitek, *Cryst. Lattice Defects* **5**, 1 (1974).
- ³⁹V. Vitek, A. P. Sutton, D. A. Smith and R. C. Pond, *Grain Boundary Structure and Kinetics*, edited by R. W. Balluffi (American Society for Metals, Metals Park, Ohio 1980), p. 115.
- ⁴⁰P. Ruterana, V. Potin, and G. Nouet, in *Nitride Semiconductors*, edited by F. A. Ponce, S. P. DenBaars, B. K. Meyer, S. Nakamura, and S. Strite, *Mat. Res. Soc. Symp. Proc. No. 482* (MRS, Warrendale, PA, 1998), p. 459.
- ⁴¹A. Béré and A. Serra, *Phys. Rev. B* **66**, 085330 (2002).